https://dx.doi.org/10.1016/j.scitotenv.2019.04.388

Aggravating O_3 pollution due to NO_x emission control in eastern China

Nan Wang [abd], Xiaopu Lyu [c], Xuejiao Deng [d], Xin Huang [ab], Fei Jiang [e], Aijun Ding [ab]

[a] Joint International Research Laboratory of Atmospheric and Earth System Sciences, School of Atmospheric Sciences, Nanjing University, Nanjing, China
[b] Jiangsu Provincial Collaborative Innovation Center for Climate Change, Nanjing, China
[c] Department of Civil and Environmental Engineering, Hong Kong Polytechnic University, Hong Kong
[d] Institute of Tropical and Marine Meteorology, China Meteorological Administration, Guangzhou, China
[e] Jiangsu Provincial Key Laboratory of Geographic Information Science and Technology, International Institute for Earth System Science, Nanjing University, Nanjing 210023, China

Abstract

China has been suffering from increasing ozone (O_3) pollution even though nitrogen oxides undergoes a notable drop during past five years. Since that O3 pollution has a nonlinear and close link to both NOx and VOC emission intensity, recent dramatic control on emissions in China would inevitably pose significant perturbations on O3 sensitivity to its precursors. To shred more light on current situation of O_3 pollution and get in-depth understandings on how to scientifically control NO_x emissions and VOCs emissions spatially and temporally, we integrated continuous satellite retrievals, ground-based measurements together with chemical transport modeling in this study. By analyzing statistical data, China has addressed much efforts in controlling NO_x emissions and NO_x emissions did decrease by ~ 25% from 2012 to 2016, corresponding to a noticeable drop in tropospheric NO_2 column concentrations in eastern China (reduced by ~ 30%). Based on multiple sensitivity simulation using a chemical transport model, we explored the characteristics and variations of O_3-NO_x-VOCs sensitivity with special focus on developed regions such as Jing-Jin-Ji (JJJ), Yangtze River Delta region (YRD) and Pearl River Delta region (PRD), respectively, in eastern China. In spatial, all the regions demonstrated the variations of O_3 sensitivities changing from VOCs sensitive dominated regimes to mixed sensitive dominated regimes, indicating O_3 formations were becoming sensitive to both NO_x and VOCs. In temporal, a diurnal shift of O_3 sensitivity existed in all the 3 regions with VOCs sensitive regimes dominated in the morning shifting to mixed sensitive dominated regimes in the afternoon. Due to the transition in O_3-NO_x-VOCs sensitivity, the diurnal peak of net O_3 formation rate was ~1-1.5h earlier in 2016 compared to 2012. Our O_3 isopleth studies suggested that relatively high levels of O_3 are in mixed sensitive regimes?? and eastern China would suffer from deteriorating O_3 pollution at least in a short-term or even in a long-term if following the past control tendency. By conducting different reduction ratios of AVOCs/NO_x scenarios, it was found NO_x-targeted emission control would lead to O_3

increments in Beijing and Shanghai, whereas VOCs-targeted control could benefits for all the three regions. The study provides scientific supports for future emission control strategy in China.

1. Introduction

Characterized by high levels of particulate matter ($PM_{2.5}$), high mixing ratio of ozone (O_3) and low visibility, air pollution in China has attracted lots of attention worldwide. In fact, China has been dedicating to fight against air pollution in the past decades. Due to the continuous efforts on emission control and restriction, the increase of $PM_{2.5}$ has been somehow mitigated and even reversed (He et al., 2017; Song et al., 2017). However, photochemical O_3 pollution is still serious (annual increasing rate is 6.5 ug/m^3 from 2013 to 2017) and frequently deteriorate atmospheric environment especially in eastern China, where highly developed city clusters such as the Beijing-Tianjin-Hebei (JJJ) area, Yangtze River Delta (YRD) region and Pearl River Delta (PRD) region are located.

Tropospheric O_3 is produced by emissions of nitrogen oxides (NO_x = NO + NO_2) and volatile organic compounds (VOCs) in the presence of sunlight (Atkinson 2000). Tropospheric O_3 is not only harmful to human health but also poses adverse impact on plants and even ecosystem (Booker et al., 2009; Fann et al., 2011; Brauer et al., 2016; Lin et al., 2018). As one of the greenhouse gases, O_3 also affects global climate (Watson et al., 1990; Shindell el al., 2004; de_Richter 2011;). The control of O_3 is of great challenge due to the complicated non-linear relationship between O_3 and its precursors (Xing et al., 2011; Ou et al., 2016). Briefly, net O_3 is accumulated when the photo-stationary reaction chains, i.e., $NO_2 + O_2 + M \leftrightharpoons NO + O_3 + M$, are unbalanced by the intervention of alkylperoxyl (RO_2) and hydroperoxyl (HO_2) from VOCs and CO, which lead to the oxidization of NO to NO_2 (RO_2 + NO + O_2 -> HO_2 + NO_2; HO_2 + NO -> OH + NO_2), and finally resulting in net O_3 accumulation via NO_2 photolysis (Atkinson 2000). The relationship between O_3 and its precursors is usually identified as VOCs-sensitive, NO_x-sensitive or mix-sensitive. In general, VOCs-sensitive regime means that reducing VOCs emissions could lead to the reduction of RO_2, which accordingly decrease the transition of NO to NO_2 and finally result in lower concentration of O_3; In NO_x-sensitive regime, cutting NO_x emissions lead to the reduction of NO_2 photolysis, causing the decrease of O1D (activated oxygen atom) which react with O_2 to generate O_3. Mix-sensitive regime has the characteristics that reducing either VOCs or NO_x emissions would result in the reduction of O_3 (Sillman., 2002; Sillman 2003; Sillman and West 2009; Sillman., 2012; Xie et al., 2014; Xue et al., 2014; Jin et al., 2015).

Current methods of mainstream to split O_3-NO_x-VOCs sensitivity covers observation-based methods, satellite retrievals and models. Usually, site observations can directly provide information of O_3 and its precursors and it is feasible to calculate O_3 sensitivity by complementing observe-based models. For example, Ling et al. (2013) investigated O_3 sensitivity in Hong Kong with a photochemical box model constrained by observed VOCs and NO_x data. The method can provide accurate in-situ diagnoses but is limited in temporal and spatial extent (Wang et al., 2017). Satellite retrievals, based on the ratio of formaldehyde (HCHO) to NO_2, are also widely used. It overcomes the limit of site measurements and provide data in time and space. Martin et al. (2004) adopted the retrievals from GOME (Global Ozone Monitoring Experient) and investigated O_3 sensitivity of Northern Hemisphere. However, the top-down observation is influenced by clouds, aerosols, precipitations and ground reflectivity thus contains uncertainties itself (De Smedt et al., 2012). Besides, most satellites provide only once-a-day observations, which could not reflect the diurnal variation. Modelling approaches, based on air quality simulations, provide explicit calculations in terms of chemical species and chemical sensitivities to precursors across time (from hourly to yearly) and space (from ~1 km to ~100 km). Though air quality model involves uncertainties from emission inventories, they are powerful regulatory tools especially in evaluating emission control strategies and policy decisions (Xing et al., 2011; Li et al., 2013; Wang et al., 2016).

In eastern China, there has been several studies conducted to explore O_3-NO_x-VOCs sensitivity. Due to the abundance of NO_x emissions from sources like transportation and local industries/plants, most previous studies concluded that urban areas are VOCs sensitive (Shao et al., 2009; Wang et al., 2009; Chou et al., 2009; Sun et al., 2011). For example, Wang et al., (2010) used the ratio of O_3 and NO_z as the indicator to split O_3-NO_x-VOCs sensitivity and reported that Beijing (in JJJ) was under a strong VOCs-sensitive regime. Ding et al. (2013) suggested that Nanjing, a developed city in YRD, was located in VOCs sensitive regimes according to observations of NO_y, O_3 and CO. Shao et al. (2009) found that urban areas of Guangzhou in PRD was also sensitive to VOCs through an observation-based model. With regard to rural areas in eastern China, studies concluded that O_3 formation was generally controlled by NO_x sensitive regimes (Wang et al., 2009; Xing et al., 2011).

Though lots of studies have been made, most of these studies were based on in-situ study or on a small region, there is few studies conducted on a mesoscale in both temporal and spatial. More importantly, most of them were conducted using earlier data, which could not reflect the current situation of China, especially after the period of 12th *Five Year Plan* (FYP， 2010-2015) and *Atmospheric Prevention and Protection Action Plan* (APPAP, 2012-2017) when intensive efforts on NO_x emission abatement were made whereas the control of VOCs emissions was almost neglected. With the rising trend of O_3 year by year, governments and policymakers are keen to know the up-to-date O_3 sensitivities. In this study, we firstly went over the past NO_x abatement policy/strategies in China. Observations, including both satellite retrievals and ground-based air quality monitoring data were combined with emission inventories to help understand NO_x abatement in China. Further, multiple numerical simulations based on a chemical transport model (CTM) was used to investigate the difference of O_3-NO_x-VOCs sensitivity between 2012 (when NOx emissions reached the peak) and 2016 (when NOx emissions noticeably reduced). The characteristics and variations of O_3-NO_x-VOCs sensitivity were compared and discussed. Finally, we probed deeply into understanding O_3-NO_x-VOCs regime in 2016 with the aim to provide theoretical support for future emission control policy making in China.

2.Method and Material

2.1 Data

We used the operational Ozone Monitoring Instrument (OMI) NO_2 product to identify tropospheric NO_2 variations in eastern China. OMI incorporates one visible region (349-504nm) and two UV region (264-311 nm and 307-383nm) with a spectral resolution between 0.42 to 0.63 nm and a spatial resolution of 13 × 24 km^2 at nadir (Levelt et al., Jin et al.,). As a nadir-viewing spectrometer, OMI provides daily global coverage product with a local time around 13:30. In this study, we used tropospheric NO_2 products between 2005-2017 (DOMINO v2.0), which were developed by the Royal Netherlands Meteorological Institute. Generally, the DOMINO retrieval involves three steps. Firstly, using Differential Optical Absorption Spectroscopy (DOAS) technique to access NO_2 slant columns from OMI instrument; Secondly, separating the tropospheric and stratospheric contribution to the slant column; Finally, using the tropospheric air mass factor (AMF) to convert tropospheric slant column into a vertical column (Boersma et al., 2004; 2007;2011). To be noted that OMI data was affected by row anomalies since 2007, the DOMINO algorithm followed the Row Anomaly Flagging Rules and discarded the affected rows which introduce pollution. More details are given by Boersma et al (2011).

Emissions of O_3 precursors, namely, NO_x and VOCs, were obtained from Multi-resolution Emission Inventory for China (MEIC, available at http://www.meicmodel.org/). MEIC refers to a series of Chinese anthropogenic emission inventories with spatial resolution of 1°×1° , 0.5° ×0.5° and 0.25°×0.25°, respectively. Developed by Tsinghua University, MEIC has been openly accessible to public since 2010 and has been keeping updated for providing recent emission benchmark in China. It involves major atmospheric pollutants including SO_2, NOx, CO, NMVOC, NH_3, $PM_{2.5}$, PM_{10}, BC and OC from sources like transportation, power plants, agriculture, residential and industry (He et al., Zhang et al.,). In this study, NOx and VOCs emissions from 2008, 2010, 2012, 2014 and 2016 were analyzed aiming to understand variations of O_3 precursors in the past. In addition, the 2012-based and 2016-based MEIC emission inventories were adopted to drive CTM modeling for the exploration of O_3 sensitivity in eastern China.

Ground-based monitoring data of NO_2 and O_3 were collected from China Statistical Yearbook by National Bureau of statics (2013-2017, available at http://www.stats.gov.cn/tjsj/ndsj/, in Chinese, last access: 23 Nov. 2018), which originated from Ministry of Environmental Protection (MEP) of China. Since 2013, national MEP had enlarged the operational air quality monitoring sites from 31 cities to 74 cities in China in order to provide more detailed monitoring information (GB3095-2012). Therefore, we showed yearly averages of NO_2 and O_3 from 74 cities between 2013-2017 in this study. Besides, hourly values of meteorological parameters (temperature, relative humidity, wind) and trace gases (NO_x and O_3) were used to evaluate model performance (site distributions are illustrated in Fig 1). Meteorological data and trace gases were obtained from operational surface monitoring stations maintained by China Meteorological Administration (CMA) and China Environmental Monitoring Center, respectively (CEMC). Our previous studies have demonstrated the good quality of these data (Wang et al., Xu et al., Huang et al).

2.2 Model and methods

In this study, a chemical transport model, i.e., Weather Research Forecast – Community Multiscale Air Quality (WRF-CMAQ) modelling system, was employed to investigate O_3 sensitivity in Eastern China. A two-nested domain was chosen with a grid resolution of 36 × 36 km and 12 × 12 km, respectively. The outer domain covered most area of China, parts of Southern China Sea and Western Pacific. The inner domain covered eastern China with JJJ, YRD and PRD being highly focused (Fig). Vertically, there were 30 sigma levels based on terrain-following hydrostatic-pressure coordinate, with the lowest level from the ground surface to the top of 100 hPa.

Table 1 Configuration and settings of WRF-CMAQ modeling system

Item	Domain1	Domain2
Number of girds	170,130	199, 256
Horizontal resolution	36 km	12 km
Microphysics	WRF single-moment 5-class microphysics	
Short-wave radiation	Goddard	
Long-Wave radiation	RRTM	
Observation nudging	Yes	
Boundary Layer	ACM2	
Gas-phase Chemistry	CB05	
Aerosol option	AERO5	
Anthropogenic Emissions	MEIC	
Natural Emissions	MEGAN	

The WRF model (version 3.9.1) was performed to simulate weather conditions by using the 1° x 1° NCEP (National Centers for Environmental Prediction) FNL Operational Global Analysis data (ds083.2). Meanwhile, the NCEP ADP Global Upper Air Observational Weather Data (ds351.0) was assimilated via nudging technique to improve meteorological simulations. The key configurations of WRF-CMAQ involved that, the Rapid Radioactive Transfer Model (RRTM) for short and long wave radiation scheme, the Noah Land Surface Model for land-atmospheric interactions, the ACM2 boundary layer scheme, the Lin microphysics scheme, the Kain-Fritsch scheme for cumulus parameterization and the Carbon Bond 05 (CB05) combined with AERO5 for gas-phase and aerosol chemistry (summarized in Table 1). Anthropogenic emission inventories were obtained from MEIC as aforementioned. Biogenic emissions including BVOCs and NO were calculated offline using the Model of Emissions of Gases and Aerosols from Nature (MEGAN, Guenther et al., 2006).

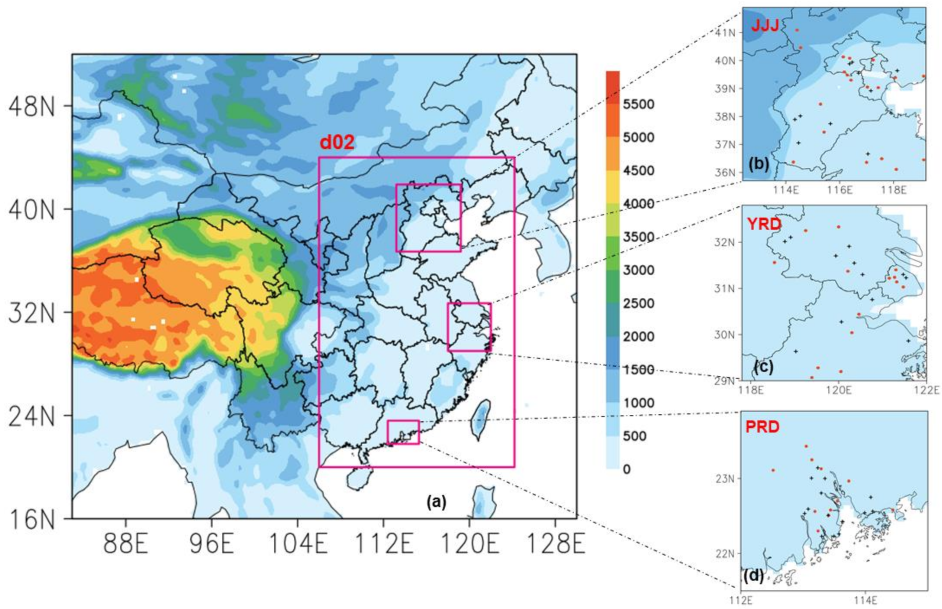

missing colorbar label

Fig 1 Modeling domains and the 3 focused regions in eastern China (a), the contour is terrain height; and JJJ (b), YRD (c) and PRD (d). The red and black dots in b-d represents air quality monitoring stations (from CEMC) and weather monitoring stations (from CMA).

We used WRF-CMAQ to investigate NO_x abatement on O_3 sensitivity during O_3 season, namely, August, when O_3 pollution gets extremely frequent throughout the country (Ding et al., 2013; 2016; Wang et al., 2017). Here, we studied O_3 sensitivity regime in 2012 and 2016 since these two year featured NO_x emission peaks and a noticeable decrease in NOx concentration, respectively. Two numerical experiments were designed, both of which shared exactly same model configuration and input except for anthropogenic emissions. Sensitivity runs were conducted using the 2012-based and the 2016-based MEIC by reducing AVOCs or NO_x emissions, respectively. In this study, O_3 sensitivity regime was identified in equivalent scenarios with 50% reductions in AVOCs and in NO_x emissions as suggested by Sillman and West (2009). The results are discussed in Section. Moreover, the relative incremental reactivity (RIR), reflecting the relative change of O_3 formation rate response to perturbations in precursors (Cardelino and Chameides, 1995), was also calculated to verify method mentioned above in diagnosing O_3 sensitivity. Usually, a larger positive RIR of NO_x (or VOCs) indicates a higher probability that O_3 production will be more sensitive to NO_x (or VOCs). The definition and verification using RIR are provided in supplementary.

Further, we conducted O_3 isopleth simulations in eastern China to improve our understanding of O_3 sensitivity in 2016. Sensitivity simulations were conducted for 10 days (Aug 20-29) which covered both O_3 polluted and non-polluted days representing a general level of O_3 season in eastern China. Generally, scenario simulations were undertaken with reducing NO_x or AVOCs emissions by 0%, 25%, 50%, 75% or 100%, respectively. In particular, more intensive reduction scenarios were conducted within the range of 0% and 50% reduction of NO_x or AVOCs emissions, aiming to provide more detailed O_3 sensitivities to precursor perturbations. As a result, we performed 40 cases as depicted in the scenario matrix (FigureS XX).

3. Result and Discussion

3.1 NO_x control in China

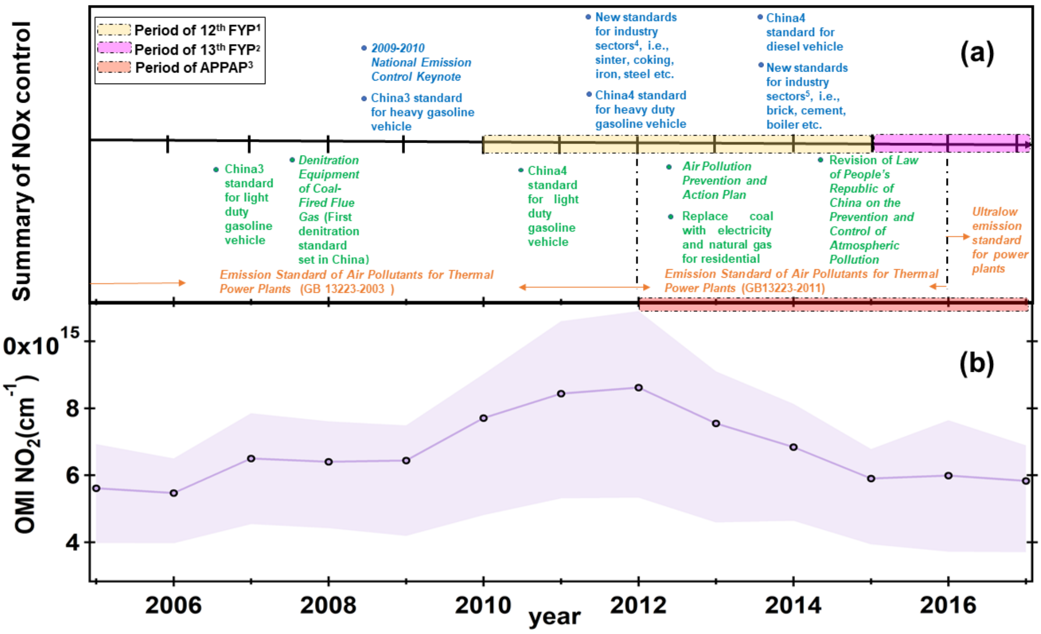

Figure 2 Timeline summarizing major NO_x emission control strategies/policies in China

[1] The 12th Five Year Plan (2010-2015), a national goal set to reduce 10% national NOx emission with a result of 18.6% reductions in national NOx emissions.

[2] The 13th Five Year Plan (2016-2020), a national goal set to reduce 15% national NOx emission, in progress.

[3] Air Pollution Prevention and Action Plan (2012-2017), aimed to reduce 25%, 20% and 15% $PM_{2.5}$ in JJJ, YRD and PRD, respectively.

[4] New standards for industrial sectors including sinter (GB28662-2012), coking (GB16171-2012), iron (GB28663-2012) and steel (GB28664-2012)

[5] New standards for industrial sectors including brick (GB29620-2013), cement (GB4915-2013) and boiler (GB13271-2014).

During the past decade in China, the control of O_3 precursors was mainly focused on NO_x emissions while there was little control on VOCs emissions. Fig 2 summarized the major progress and milestone of NO_x emission abatement policies/strategies during past decade in China. Generally, the whole period can be divided into two phases. The first phase (2005-2011) is characterized by dramatical increases in NO_x emissions. Statistical results showed that NO_x emissions were 19.48 Mt in 2005 while the amount accelerated to 26.05 Mt (1.33 times higher) in 2010 (Zhao et al., 2013). Observations from satellite instruments also confirmed this increment, tropospheric NO_2 column depicted an increasing rate of 5×10^{14} molecules/cm^2 per year between 2005 and 2011 (Fig 1b). The increment could be attributed to that, on one hand, NO_x emissions control within this period merely considered automobiles and power plants, the emission standards were relatively comfortable with GB13223-2003 for power plants and China III standard for vehicles (Fig.1a). On the other hand, there had been a noticeable increase of new-built power plants and automobile amount, which turned up by 195% and 300% according to Wang et al., (2012). To mitigate air quality, Chinese government has taken more ambitious steps to control NO_x emissions in the second phase. The 12^{th} Five Year Plan (FYP) pledged to reduce NO_x emissions by 10% between 2010 and 2015, which was a first national goal set for NO_x emission abatement. In particular, a more tightened standard (GB13223-2011) was put into force for power plants since 2012. The limit value of NO_x emissions was strengthened to be 100 mg/m^3 compared to the value of 450-1100 mg/m^3 based on the previous standard (GB13223-2003). In 2013, the State Council issued "Air Pollution Prevention and Action Plan" (APPAP), symbolizing the campaign entered into a more aggressive state. The plan aimed to reduce 25%, 20% and 15% $PM_{2.5}$ in JJJ, YRD and PRD between 2012 and 2017, respectively. As one pollutant co-emitting with primary particle and also one major precursors of $PM_{2.5}$, NO_x emissions would be inevitably controlled. Indeed, more stringent control measures were undertaken. For example, phasing out high-emitting industries, closing small/outdated factories, eliminating yellow label car, tightening industrial emission standard, improving fuel quality, speeding up the adjustment of energy structure, using laws/standards to force industrial transformation or upgrading and etc denitration? (Fig. 2a). Furthermore, ultra-low emission standard was initiated for large power plants since 2016, with NOx emission limit setting to 50 mg/m^3. As a result, tropospheric NO_2 column concentrations in the second phase (2012-2016) decreased by ~31%, with the decreasing rate of -6×10^{14} molecules/cm^2 per year.

By investigating NO_x emissions, we found similar variations (Fig 3). An increasing trend was found between 2008 and 2012 (increased by 21.1%). The annual NOx emissions in 2012 reached 29.2×10^6 Ton, which was the peak during the last decade. After 2012, a decreasing trend was seen with the annual NOx emissions reduced to 22.5×10^6 Ton in 2016 (reduced by 23%). It could be found that power plant was the sector with the most reduction of NO_x emissions, which took up 66.5% of NOx emission reductions from 2012 to 2016, followed by industry (18.6%), transportation (11.7%) and residential (3.1%), respectively. The noticeable NO_x emissions reductions were consistent with tropospheric NO_2 column variations demonstrated in Fig 1b. Compared to NO_x emissions, VOCs emissions showed a slightly increase in the last decade because of the lack of available VOCs emissions control in China. Fig 3 showed that VOCs emissions were increased between 2008 and 2012 and then maintained in a relatively stable level between 2012 and 2016. The annual VOCs emissions were 23.6×10^6 Ton, 28.1×10^6 Ton and 28.4×10^6 Ton in 2008, 2012 and 2016, respectively.

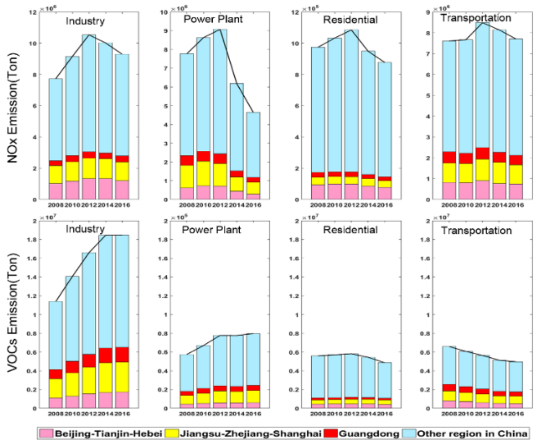

Figure 3 NO_x and anthropogenic VOCs emissions from industry, power plant, residential and transportation from 2008 to 2016 in China.

Accordingly, surface monitoring data depicted that ambient NO_2 concentrations decreased by 11.4% from 2013 to 2016 (Fig 4), reflecting that the NO_x emission control had taken good effect in China. However, ambient O_3 concentrations showed an opposite trend, with annual concentration increased from 139 ug/m^3 in 2013 to 167 ug/m^3 in 2017. The increasing rate was 6.5 ug/m^3 per year, indicating that photochemical pollution has becoming more and more stringent in China. Indeed, O_3 problems have been frequently addressed by others (Atkinson et al; Cheng et al., 2010; Shao et al., 2009; Ding et al 2013; Wang et al., 2017;).

Based on the analyses aforementioned, China has achieved some effects in NOx emission control while is facing a more serious O_3 problem. As major precursors of O_3, the changes of NOx emissions would directly affect the mechanism of O_3 formation. To ensure efficient abatement for O_3 control in future work, it is of great importance to distinguish the variations of O_3-NOx-VOCs sensitivity and perceive the up-to-present characteristics in China.

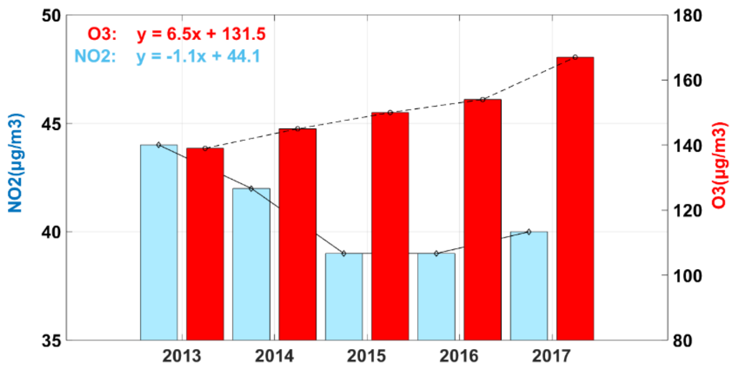

这里可以分区域，和你后面的模拟讨论区域对应，再加三个小图

Figure 4 Variations of surface monitored O_3 and NO_2 in 74 cities from 2013 to 2017

3.2 Responses of O_3 to NOx/VOCs emission perturbations

Table 2 Statistical comparisons of simulated and observed parameters

Region	**Parameter**	**Obs$_{mean}$**	**Sim$_{mean}$**	**MB**	**NMB**	**NME**	**RMSE**	**IOA**
JJJ	T (°C)	25.9	25.2	-0.74	-0.02	0.06	2.14	0.92
	RH (%)	75.1	73.3	-1.75	-0.02	0.11	10.60	0.89
	WS (m/s)	1.9	2.8	0.9	0.57	0.71	1.53	0.61
	O_3 (ppb)	34.1	33.2	-0.9	-0.01	0.45	19.4	0.84
	NO_2 (ppb)	13.0	18.2	5.2	0.38	0.7	12.7	0.63
YRD	T (°C)	29.3	28.5	-0.8	-0.03	0.05	2.06	0.91
	RH (%)	74.8	79.6	4.8	0.06	0.11	10.16	0.86
	WS (m/s)	2.1	3.1	1.0	0.74	0.86	1.52	0.63
	O_3 (ppb)	39.5	31.5	-8.0	-0.22	0.46	0.84	0.86
	NO_2 (ppb)	14.1	27.7	13.6	1.16	1.06	19.2	0.52
PRD	T (°C)	28.7	29.0	0.2	0.01	0.04	1.63	0.91
	RH (%)	83.5	82.6	-0.9	-0.01	0.07	8.21	0.88
	WS (m/s)	2.2	3.1	0.9	0.46	0.65	1.78	0.69
	O_3 (ppb)	31.0	29.3	-1.7	-0.04	0.46	19.2	0.87
	NO_2 (ppb)	12.9	18.7	5.8	0.44	0.85	15.2	0.60

We firstly present the evaluation of WRF-CMAQ model before exploring O_3 sensitivity. Hourly observed data collected from CMA (temperature, relative humidity and wind) and CEMC (trace gases) were used to compare with those simulated. As summarized in Table 2, statistical calculations, including mean values (Obs$_{mena}$ and Sim$_{mean}$), mean bias (MB), normalized mean bias (NMB), normalized mean error (NME), root mean square error (RMSE), and the index of agreement (IOA), were introduced for validations. It was found that all the meteorological parameters showed high values of IOA (Table 2) in JJJ, YRD and PRD, respectively, indicating the good trend between observations and simulations. Meanwhile, the magnitudes were also well matched as the biases were relatively small (i.e., NMB, NME and RMSE). Therefore, the simulated weather conditions were well reproduced.

Simulated O_3 and NO_2 (Table 2) were also verified with field measurements. The mean bias of O_3 in JJJ, YRD and PRD were 5.2 ppb, -8.0 ppb and 5.8 ppb with IOA value equaled 0.84, 0.86 and 0.87, respectively, showing good simulations of O_3. The simulations of NO_2 were slightly overestimated with MB of 5.2, 13.6 and 18.7 in JJJ, YRD and PRD, respectively. One possible reason was that NO_2 could be directly affected by local emissions in urbans, i.e., mobile vehicles, and such sources were a weakness of emission inventories. Besides, our model had the finest horizontal resolution of 12 km×12 km, thus it was difficult to reflect the topographic-induced effects which might affect air pollutants (Wang et al., Li et al., Jiang et al.,). Since the aim of the study is to reflect general conditions based on monthly scales, relatively well simulations of the trends and magnitudes could meet the demand. Moreover, by comparing with previous modeling studies, our results were within the typical ranges and thus could be accepted for further analyses (Ding et al., Huang et al. 2016, Wang et al., XXXX).

Fig 5 Shows the results of modeled O_3 using different year-based emission inventories under multi scenarios, namely, baselines, 30% and 50% reductions in NOx and VOCs emissions in 2012 and 2016, respectively.

By exploring the spatial distributions of O_3 in 2012 (Fig 5a), relatively high levels of O_3 concentrations could be found in JJJ, YRD and PRD, with the monthly area mean concentrations of 68 ppb, 69 ppb, and 61 ppb, respectively. When it came to 2016, area mean concentration of O_3 in these 3 areas increased by 2.8 ppb, 3.7 ppb, and 4.1 ppb, respectively. The increments were consistent with the increasing trends of monitored O_3 in Fig 4.

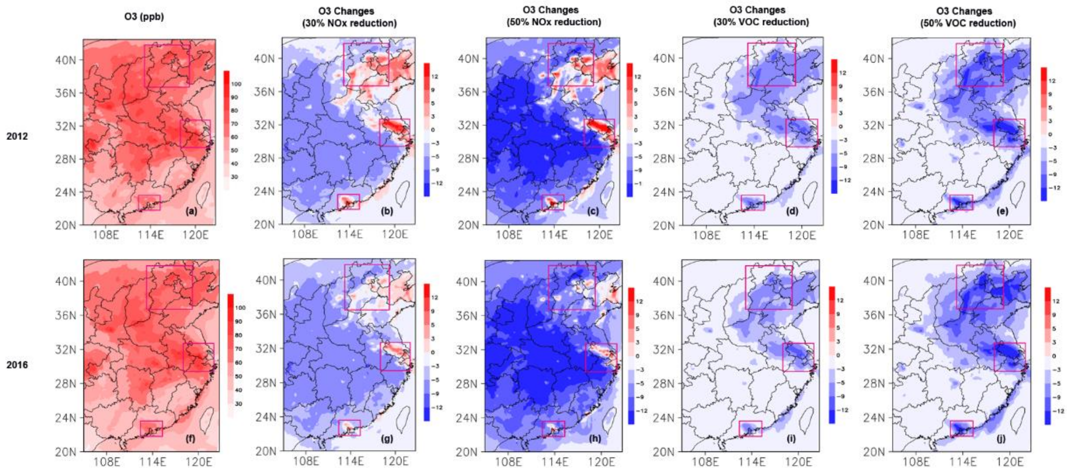

Figure 5 Spatial distribution of max O_3 in 2012 and 2016 (a and f), respectively; O_3 changes due to perturbations of NOx emissions (b, c, g, h) and VOCs emissions (d, e, i, j) in 2012 and 2016, respectively.

For the year of 2012, 30% reduction of NOx emissions led to O_3 increments in most areas in JJJ, YRD and PRD, respectively (Fig 5b). Though several reduced areas (mainly rural areas) existed within the 3 regions, the area mean concentrations of O_3 increased by 7.4%, 3.0% and 8.3% in JJJ, YRD, and PRD, respectively. On the other hand, large areas of O_3 decreases could be found in most of the rest eastern China (reduced by 10%) such as the central, the southwestern and the northwestern (these areas were defined as the rest areas in this paper). The responses became more significant both in the increased areas and the reduced areas if 50% NO_x emissions were reduced (Fig 5c). Under the 50% NO_x emission reduction scenario in 2012, O_3 would be increased by 6.4%, 2.0% and 7.5% in JJJ, YRD and PRD, and decreased by 19.2% in the rest areas, respectively. Such responses implied that VOCs sensitivity controlled in most areas of the 3 developed city clusters, while NO_x sensitivity dominated in the rest areas. In terms of 2016, the rebounds of O_3 due to NOx reductions shrank significantly in the 3 city clusters (see red areas in Fig 5g and Fig 5h). The increments of O_3 became weaker, with O_3 area mean changed by 1.1%, -1.4% and 0.5% in JJJ, YRD and PRD, respectively, in the 2016-based 30% NOx reduction scenario. And O3 rebounds even turned to negative in the 2016-based 50% NOx reduction scenario, with O_3 area mean changed by -3.2%, -8.2% and -4.5% in JJJ, YRD and PRD, respectively. Such variations implied that O_3 sensitivities in these developed areas had somehow changed in 2016. When it came to O_3 responses to VOCs emissions, areas showed sensitive to VOCs emissions were North China Plain (including JJJ), YRD and PRD. In 2012, the 30% VOCs reduction scenario showed that O_3 decreased by 10.8%, 9.6%, and 12.0% in JJJ, YRD and PRD, respectively. And the decrease became 14.8%, 14.0% and 17.8%, respectively, in terms of the 50% VOCs reduction scenario in 2012. Similar variations could also be found in 2016 (Fig 5f and Fig 5j), indicating that these areas were VOCs sensitive or at least mixed-sensitive. However, the rest areas showed little sensitive to VOCs emission perturbations with △O_3 less than 2 ppb under all the VOCs reduction scenarios, which confirmed the conjectures, namely NO_x sensitive, regarding to the analyses of NO_x emission perturbations.

By considering O_3 responses to NO_x and VOCs emission reductions together, a common reducing area was found mainly located ~32°N-36°N of the east, implying a mix-sensitive area. Moreover, it might be inferred that JJJ, YRD and PRD were changing from a VOCs-sensitive dominated regime to a mix-sensitive dominated regime from 2012 to 2016 given the shrunken signals of O_3 rebounds due to NO_x emission reductions and the responses of O_3 to VOC emission perturbations as well.

3.3 Transition of O_3-NO_x-VOCs sensitivity regime

In order to quantitatively identify the effect of NO_x emission abatement on O_3-NO_x-VOCs sensitivity in eastern China, the method proposed by Sillman and West (2002) were taken. Locations of O_3 sensitivity were classified to NO_x sensitive, VOC sensitive, mixed sensitive, NO_x titration and no sensitive regimes. In particular, a location is defined as NO_x sensitive (VOCs sensitive) regime if O_3 decreases at least 5 ppb because of reducing NO_x emissions (VOCs emissions) and the decrease of O_3 due to NO_x emission reductions (VOCs emission reductions) is at least twice as large as the decrease due to reduced VOCs emissions (NO_x emissions). A place is treated as mixed sensitive regime if O_3 declines by more than 5ppb in response to either reducing VOCs or NOx emissions and the reduction of O_3 due to VOCs emission reductions and NOx emission reductions differ by less than a factor of two. A site is controlled by NOx titration if the O_3 increments are over 5 ppb due to NOx emission reduction and O_3 decreases less than 5 ppb due to VOC emission reductions. Finally, a site is considered to be no sensitive regime if O_3 decreases less than 5ppb in response to either VOCs emission or NO_x emission reductions. Furthermore, an additional method using RIR of NOx (VOCs) emissions was also introduced to evaluate the results. The comparisons were provided in FigS XX. The diagnosed patterns agreed well with each other indicating a convincible result by using the method from Sillman and West. (Detailed discussion were provided in supplementary file)

3.4.1 Spatial variations and characteristics

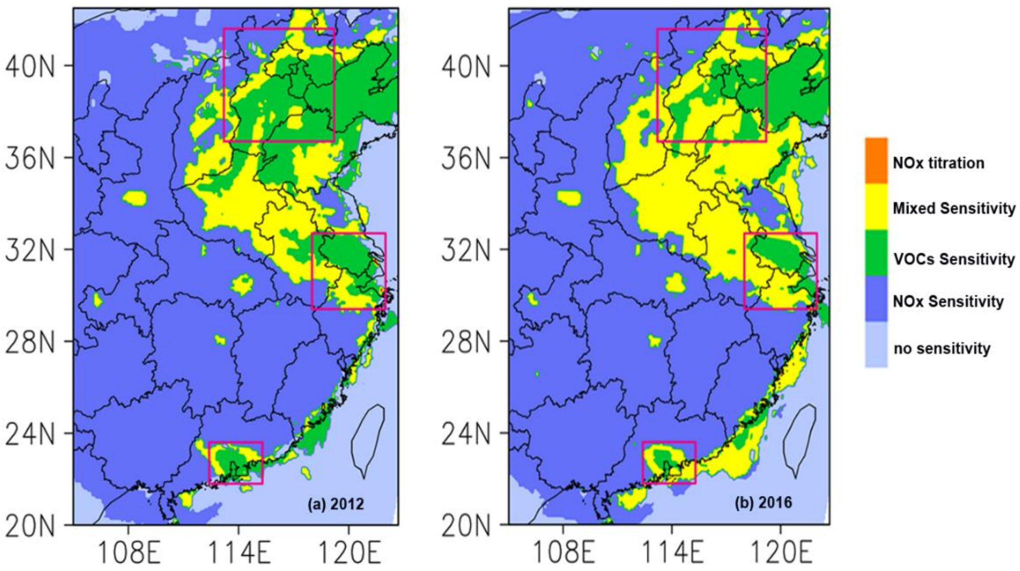

Figure 6 Spatial comparison of O_3-NO_x-VOCs sensitive regime between 2012 and 2016 in eastern China

By comparing O_3 sensitivities between 2012 and 2016, noticeable changes were observed in JJJ, YRD and PRD, respectively (Fig 6). In 2012, a widespread VOCs sensitive regime was found over the 3 regions, and a NOx sensitive regime was dominated in the rest areas. In terms of 2016, however, mixed sensitive regimes seemed to draw equal with VOCs sensitive regimes or even dominated in the 3 regions. Besides, similar changes were also observed in Shandong province, a part of North China Plain. In JJJ, the percentage of total grids occupied by VOC sensitive regime reduced from 63.1% in 2012 to 40.0% in 2016 whereas that of the mixed sensitive increased from 25.0% in 2012 to 44.1% in 2016. Though the percentages of VOCs sensitive regimes were shrunken in 2016, VOC sensitive regimes were still found in central Beijing, Tianjin, Tangshan and some other cities in Hebei

Province. These cities are characterized by relatively high NO_x emissions likely from mobile vehicles or power plants. In YRD, the percentage of mixed sensitive regime increased from 31.4% in 2012 to 52.2% in 2016. In particular, mixed sensitive regimes were seen in cities such as Hangzhou, Nantong, Ningbo, Jiaxing and other cities in Zhejiang province after NOx emission abatements. However, VOC sensitive regimes were still found in some developed urban cities, such as Shanghai, Suzhou, Wuxi, most of Nanjing and other cities in Jiangsu Province. Moreover, a few grids indicating NO_x titration occurred in 2012 disappeared in 2016. Usually, grids depicting NO_x titration regimes refer to places close to high NO_x emissions sources, such as industries/power plants, the disappearances of NOx titration regimes implied the efforts of industrial transformations made in YRD. In PRD, the 2016-year pattern demonstrated that both VOCs sensitive regime (21.0%) and mixed sensitive regime (50.3%) controlled in Guangzhou, Shenzhen, Dongguan and Foshan, while NO_x sensitive regimes dominated in rest cities of PRD. Moreover, clear differences were also found in those receptors of downwind areas, for example, coastlines. O_3 sensitivities along these areas were also changed from VOCs sensitive regimes to mixed sensitive regimes.

Previous studies based on observations (in-situ observations or satellite observations) and models have been conducted to study O_3 sensitivities in eastern China (Table 3). Generally, our diagnosed results matched well with those results in eastern China. Specifically, Jin et al., (2015) employed OMI observations ($HCHO/NO_2$) to split O_3 sensitivity and found that transitional regimes (mixed sensitive) dominated in most areas of JJJ, YRD and PRD, respectively, whereas we found both VOCs sensitivity and mixed sensitivity were the dominated regimes. The discrepancy between the two studies can be attributed to the following aspects. One possible reason is that satellite measurements are based on optical properties which are affected by clouds, aerosols, precipitations, and surface reflectivity. The observation contains uncertainties itself. For example, the uncertainty of HCHO products range from ~30% to 40% according to De Smedt et al., (2012). Besides, satellite observations provide vertical column concentrations which are different to ground-level concentrations (Boersma et al., 2004). More importantly, our further analysis showed that O_3 sensitivities depicted diurnal changes in the three regions with a shift of VOCs sensitive in the morning to mixed or NOx sensitive in the afternoon (details refer to Section 3.4.3). In fact, OMI observations only provide once-a-day observations and are limited to the early afternoon conditions (Jin et al., 2015).

Table 3 Comparisons with previous O_3 sensitivity studies

Study area	Site info	Study time	Method	O_3 sensitivity	References	This study
Beijing	Birds Nest, urban;	07-09 2008；	ΔOx/ΔNOz;	VOC-limited;	Sun et al., (2010)	VOC-limited in central areas and mixed-limited in suburban/rural
	PKU (urban);	08.2014;	VOC/O_3;	VOC-limited;	Shao et al., (2008)	
	Urban and rural;	07.2005;	CMAQ-RSM;	urban: VOC-limited, rural: NOx-limited;	Xing et al., (2011)	
	Whole area;	2013 Summer;	Satellite retrievals;	mixed-limited in most area	Jin et al., (2015)	
Tianjin	Urban;	07-08 2010;	NCAR_MM;	mix-limited;	Ran et al., (2012)	VOC-limited dominated
JJJ	Whole area	2015	CMAQ-ISAM;	VOC-limited in urban and mixed/NOx-limited in suburban/remote;	Han et al., (2018)	VOC-limited in urbans and mixed-limited in suburban/rural
	Whole area	2013 Summer	Satellite retrievals (HCHO/NO2)	Transitional dominated	Jin et al., (2015)	
Nanjing	SORPES (suburban);	2011-2012;	ΔO_3/ΔNOy;	VOC-limited;	Ding et al., (2013)	VOC-limited dominated
	SORPES (suburban);	10. 2014;	OBM (MCM);	VOC-limited;	Xu et al., (2017)	
	4 urban sites	06-08 2013;	OBM (CB4);	VOC-limited;	An et al., (2013)	
Shanghai	Xujiahui (urban)	07-08 2009;	NCAR_MM;	NOx-inhibited;	Ran et al., (2012)	VOC-limited
	Urban	2006-2007;	NCAR_MM;	VOC-limited;	Geng et al., (2008);	
	Urban	09. 2009	WRF-Chem	VOC-limited	Tie et al., (2012)	
	Rural and urban	07. 2007	CMAQ;	Urban: VOCs-limited; Rural: NOx-limited	Li et al., (2011)	
Hefei	Whole area	2015-2017	Satellite retrievals;	NOx-limited;	Sun et al., (2018)	NOx-limited
YRD	Whole area	2013 Summer	Satellite retrievals (HCHO/NO2)	Transitional dominated	Jin et al., (2015)	VOCs-limited and mixed-limited dominated
Guangzhou	WQS (suburban)	10-12 2007	OBM (MCM);	VOCs-limited	Cheng et al., (2010)	VOC-limited and mixed limited
	Urban	2000	OBM;	VOCs-limited	Shao et al., (2009)	
	Urban and suburban	2006 Summer;	OBM(CB4);	Urban: VOCs-limited Suburban: NOx-limited	Lu et al., (2010)	
Zhuhai	Wanshan (suburban)	2013 Autumn	PBM-MCM	Transitional (Mixed)	Wang et al., (2018)	Mixed limited;
PRD	Whole area	2012	CMAQ	Urban: VOCs-limited Remote: NOx-limited	Wang et al., (2017)	Urban: VOCs-limited and mixed limited；
	Whole area	2013 Summer	Satellite retrievals (HCHO/NO2)	Transitional dominated	Jin et al., (2015)	Remote: NOx-limited

3.4.2 Diurnal variations and characteristics

We compared net O_3 formation rate between 2012 and 2016 (Fig 7). Net O_3 formation rate is calculated considering both O_3 production rate and O_3 destruction rate. In this study, O_3 production rate is retrieved from reactions of RO2+NO and HO2+NO, whereas O_3 destruction mainly considers reactions of O1D+H2O; O_3+HO2; O_3+OH; NO2+OH; and O_3+VOCs. The difference of O_3 production rate and O_3 destruction rate is net O_3 formation rate. Similar method has been found in Wang et al., (2018). In this study, the Integrated Reaction Rate (IRR) module incorporated in CMAQ was triggered to acquire the above gas-phase reaction rates.

It was found that peak O_3 formation rate was about 1.5~3ppb/h higher in 2016 than that in 2012. The change was reasonable as VOCs sensitive regime dominated in the 3 regions in 2012, and abating NO_x emission in China led to the rebound of O_3 formation. Meanwhile, NO_x emission control resulted in the peak hour of net O_3 formation rate in 2016 about 1 ~ 1.5 hour earlier than that in 2012. In fact, O_3-NOx-VOCs sensitivity had diurnal variations changing from VOCs sensitive regime in the morning to mixed sensitive regime in the afternoon (as discussed in Fig 8). The abatement of NO_x emissions in China has resulted in more mixed sensitive regimes within the 3 regions (see Fig 6) and the O_3 peak hour usually occurs in 13:00 ~ 15:00 when mixed sensitivity dominated. The mixed dominated regimes led to the 1 ~ 1.5 hour earlier shift in 2016.

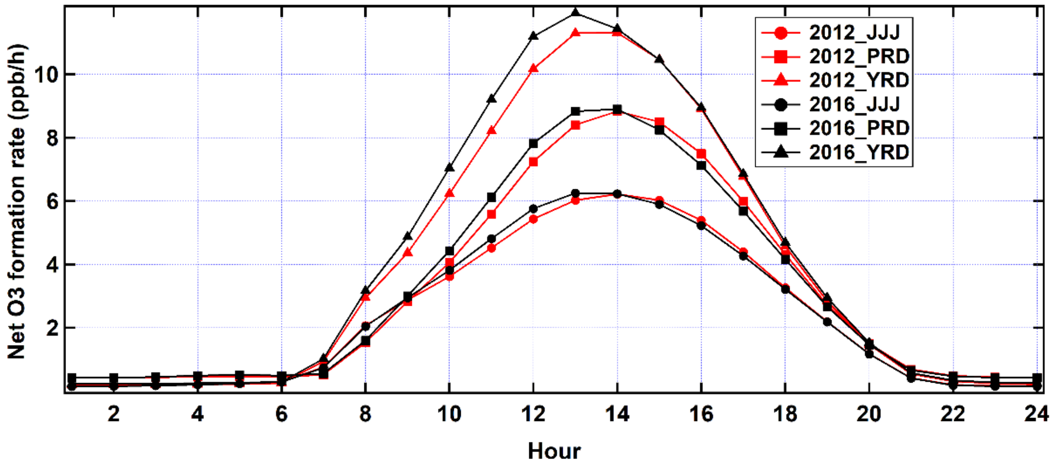

Figure 7 Comparison of O_3 net formation rate. (Net O_3 rate[1*] is calculated using O_3 production rate[2*] to minus O_3 destruction rate[3*])

[1*]Net O_3 rate= production rate – destruction rate;

[2*]production rate considers reactions of: RO2+NO; HO2+NO;

[3*]destruction considers reactions of: O1D+H2O; O_3+HO2; O_3+OH; NO2+OH; O_3+VOCs (ISOP/TOL/ETH/IOLE)

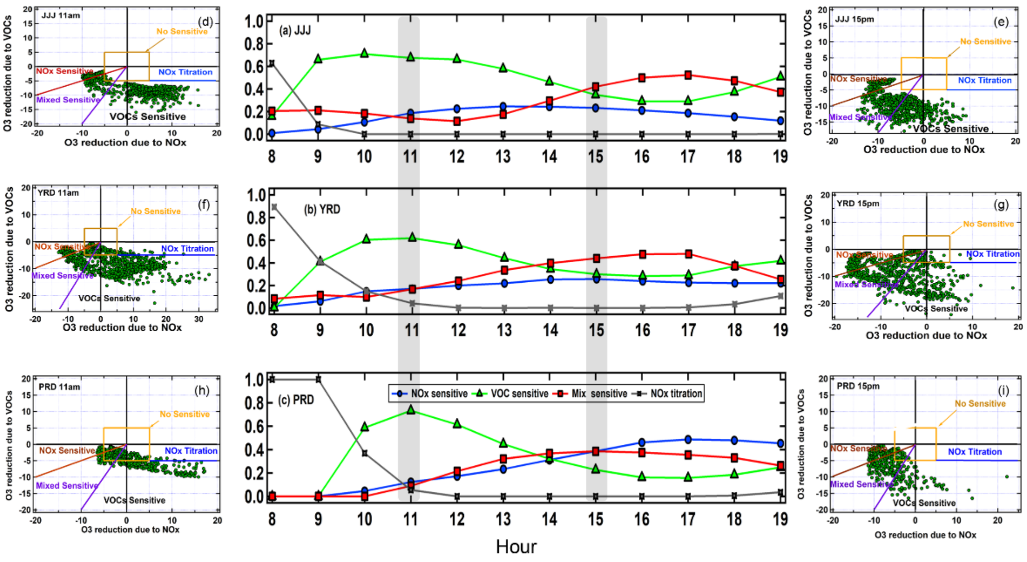

Figure 8 Percentages of O_3-NOx-VOCs sensitive regime in 3 regions from 08: am to 19:00 pm (a-c). The grey shades highlight time at 11:00 am and 15:00 pm, respectively. Model grids sorted by precursor sensitivity at 11:00 am (d, f, h) and 15:00 pm (e, g, i) in 3 regions.

Fig 8 illustrated the diurnal variations of O_3 sensitivity in 2016. All of the three regions showed similar diurnal variations. Before 8:00 am, O_3 was consumed via NOx titration. As the boundary layer gradually increased, O_3 formation tended to be VOCs sensitive in most of model grids in the morning. When it came to noon time (O_3 peak hours), mixed sensitive regimes took over and last till the late afternoon. In particular, O_3 formation turned to be NOx sensitivity in the afternoon in most PRD grids which was not seen in the other 2 regions. Compared to JJJ and YRD, the effective control of NOx emissions was earlier and could be traced back to 2003 due to the joint efforts of Guangdong government and Hong Kong government (Zhong et al and Wang et al., 2017). In addition, by comparing model grids sorted by precursor sensitivity at 11:00 am and 15:00 pm (Fig 8d-Fig 8i), in JJJ, YRD and PRD, we found grids controlled by VOCs sensitivity took up 65%, 61% and 73% at 11:00 am, respectively, and grids controlled by mixed sensitivity became 42%, 45% and 40% at 15:00 pm, respectively. The diurnal shift might be possibly due to that, the boundary was relatively low, together with an increase of NOx emissions during rush hours in the morning; and NOx emissions was gradually consumed after boundary layer expansion; besides, biogenic VOCs turned to increase in the afternoon (Ding et al., Huang et al., Sillman et al., Atkinson.,). Such diurnal variations indicate that the O_3 sensitivity of a certain site at a given hour do not apply to other times. Therefore, it brings difficulty to formulate an effective O_3 control scheme. On one hand, controlling VOCs emissions would be very effective in the morning while it might be not as that effective as in the afternoon. On the other hand, controlling NOx emissions had already elevated O_3 concentrations in some urban cities in eastern China but it seemed to be helpful for reducing afternoon O_3 concentration. Considering the complicated non-linear relationship between O_3 and its precursors, we further investigated O_3 isopleth in JJJ, YRD and PRD.

3.4 O_3 Implications for O_3 mitigation

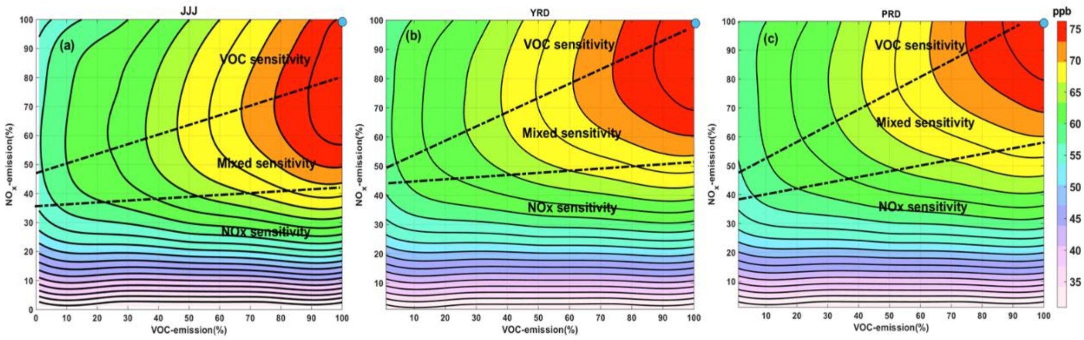

Figure 9 O_3 isopleth in JJJ, YRD and PRD, respectively.

The relationships of O_3, NOx and VOCs are shown in Fig 9. In this study, O_3 isopleth was achieved by using linear regressions from 40 scenarios based on 10-day simulations (Aug 16 -25). The selected periods covered both non O_3 polluted days and O_3 polluted days, thus could be regarded as general conditions in JJJ, YRD and PRD, respectively. In Fig 10, the VOCs sensitive, mixed sensitive and NO_x sensitive regimes, corresponded to the maximum 1-hour O_3 concentration for given precursors, were separated by ridge lines (Ou et al., 2016). To be noted that the base scenarios were at the upper right corner (red dots) and represented the benchmarks without any NOx or VOCs emission reductions. It could be found that all the base scenarios in YRD and PRD were within the area of the mixed sensitive regimes, indicating that O_3 formation was sensitive to both VOCs and NOx. With regard to JJJ, the base scenario was above the ridge line, meaning a VOCs sensitive regime dominated, while it was not far away to the mixed sensitive regime. Though the O_3 isopleths were based on 10-day simulations, the results of base scenarios were generally consistent with the monthly analyses in Fig 6, confirming again the convincible results.

Another important finding in Fig9 (a-c) is that relatively high O_3 mixing ratios are gathered within the bands of mixed sensitive regimes in all of the 3 regions, which could explain the current high O_3 levels monitored in recent year. In fact, a nationwide control against NOx emissions have been taken steps while VOCs emission controls are ignored in the past. This means that developed regions, particularly JJJ, YRD and PRD in eastern China, are suffering from VOCs sensitive regimes to the high-O_3-level mixed sensitive regimes at least in a short-term. Suppose past control tendency is maintained in the future (NOx control only), China would experience a long time suffering from high O_3 mixing ratio as the band of mixed sensitive regime is rather wide. However, if VOCs emissions could be somehow controlled then followed by NO_x abatements, the band of mixed sensitive regime turns to be narrower. Therefore, to provide scientific support for future emission control, we further explore the co-benefit based on NO_x and VOCs reductions.

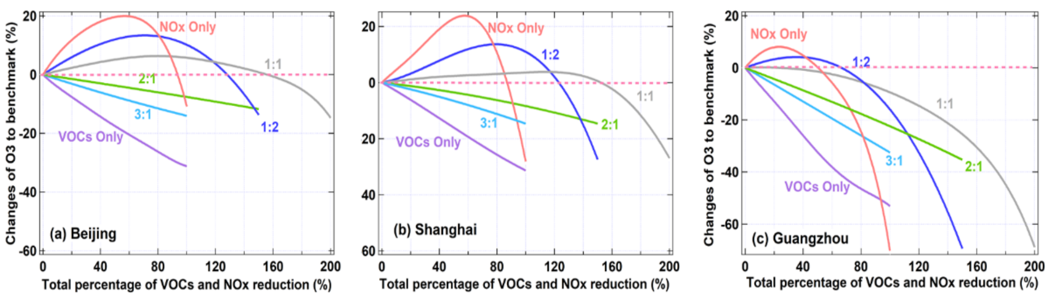

Figure 10 Changes O_3 due to different reduction of AVOC/NOx in Beijing, Shanghai and Guangzhou.

Three typical cities, Beijing, Shanghai and Guangzhou, within the 3 regions were selected to study the changes of O_3 to different degrees of precursor reductions (Fig 10a-b). Six reduction schemes were included, with AVOC/NO_x reduction ratio equaled to 3:1, 2:1, 1:1 and 1:2, the NO_x emission reduction scenario (NO_x Only), and the VOCs emission reduction scenario (VOCs Only), respectively. The horizontal axis in Fig 10a-b referred to the total reduction percentage of combined NOx and AVOCs emissions. For example, a reduction of 120% in the horizontal axis indicated that 120% reduction of NO_x and VOCs emissions with AVOC/NO_x equaled to 3:1, 2:1, 1:1 or 1:2, or with only 120% NO_x emission reduction for NOx Only and with only 120% VOCs emission reduction for VOCs Only, respectively. The results of NO_x Only scenarios in Beijing, Shanghai and Guangzhou were consistent with the analyses in JJJ, YRD and PRD, respectively. Controlling NOx emissions would degrade air quality with O_3 increments at least in the short-term, unless about more than 80% NOx emission reductions could be made in Beijing and Shanghai. Similar responses could be found for scenarios with the AVOC/NO_x=1:2 and 1:1. It should be noted that the reversal of O_3 increments in Guangzhou could be met with relatively less efforts for those NOx-focused scenarios. The 1:1 abatement scenario was an example that Guangzhou could benefit in a short-term. Furthermore, things became more promising for the scenarios with AVOC/NOx = 2:1 and 3:1, and also the VOCs Only. All of the three cities demonstrated various degrees of O_3

reduction. Speaking in a short-term, VOCs Only received the best profits for O_3 control, followed by the 3:1 scenario and the 2:1 scenario. Due to the fact that most urban areas of east China are changing from VOCs sensitive regimes to mixed sensitive regimes, it is strongly suggested that governments take VOCs-focused control in the future.

4. Summary and conclusions

O_3 problems in China are becoming more stringent and have attracted worldwide attentions. In past years, China has implemented a serious of emission control measures, particularly with a focus on NO_x emission control. As key precursors of O_3, changes of NO_x emissions would inevitably influence O_3 formation mechanism. A scientific control against O_3 needs our understandings whether to control NOx emissions, VOCs emissions or both spatially and temporally. From here, the study went over the past decade NO_x-focused emission control strategies in China, analyzed concerning statistical data and used numerical simulations to investigate the variations and characteristics of O_3-NO_x-VOCs sensitivity in eastern China.

With an increasing rate of 5×10^{14} molecules/(cm^2·year) from 2005 to 2011, tropospheric NO_2 column concentration reached the peak in 2012, then a noticeable drop (declined by ~31%) was seen between 2012 and 2016. Consistently, NOx emission data also dropped ~ 25% during the same periods. The effective NO_x abatement was due to the stringent emission control measures represented by the nationwide policy plans like *FYP* and *APPAP*. However, monitored O_3 mixing ratios have increased and are about 20.1% higher in 2017 than in 2013 (rising rate = 6.5 ug/m^3·year), suggesting O_3 pollution is becoming more stringent even though NO_x emissions is reduced.

A regional chemical transport model, WRF-CMAQ, was employed to explore the variations and characteristics of O_3-NO_x-VOCs sensitivity in east China with special focus on developed regions such as JJJ, YRD and PRD. The simulations in perturbating of NO_x and VOCs emissions indicated that most of the inland areas, for example the central, the southwestern and the northwestern of eastern China were sensitive to NO_x emissions, whereas those eastern developed areas, for example, JJJ, YRD and PRD, were sensitive to VOCs or both emissions. By qualitatively diagnosing O_3-NO_x-VOCs sensitivity, we found JJJ, YRD and PRD were changing from VOCs sensitive dominated regimes to mixed sensitive dominated regimes. For example, total grids occupied by mixed sensitive regimes in JJJ, YRD and PRD increased from 25.0%, 31.4% and 30.1% in 2012 to 42.1%, 52.2% and 50.4% in 2016, respectively. In temporal, a diurnal shift of O_3 sensitivity existed in all the 3 regions with VOCs sensitive regimes dominated in the morning shifting to mixed sensitive dominated regimes in the afternoon. In particular, PRD demonstrated NO_x

sensitive regimes dominant in the afternoon. Due to the changing of O_3-NO_x-VOCs sensitivity, the diurnal peak of net O_3 formation rate was ~1-1.5h earlier in 2016 compared to 2012.

In an attempt to provide scientific support for future O_3 control, we conducted O_3 isopleth study. The results suggested that relatively high levels of O_3 were in mixed sensitive regimes. The up-to-now conditions in JJJ, YRD and PRD are situated in (or close to) the relatively wide zone of mixed sensitive regimes. This means that China would suffer from high O_3 concentrations at least in a short-term or even in a long-term if following the past control tendency. By conducting different reduction ratios of AVOCs/NO_x scenarios, it was found NO_x-focused emission control would lead to O_3 increments in Beijing and Shanghai. At last, it is strongly to apply VOCs-focused control measures in future control as all the three regions could receive benefits in terms of O_3 control.

Acknowledgement

This study is supported by…. The author also show thanks Tsinghua University for sharing MEIC.

Reference

Watson R T, Rodhe H, Oeschger H, et al. Greenhouse gases and aerosols[J]. Climate change: the IPCC scientific assessment, 1990, 1: 17.